

## STUDIES OF HELIUM GAS MIXTURES IN DRIFT CHAMBERS\*

Patricia R. Burchat and John Hiser

Santa Cruz Institute for Particle Physics  
University of California, Santa Cruz, CA 95064

Adam Boyarski and Don Briggs

Stanford Linear Accelerator Center  
Stanford University, Stanford, CA 94309

### Abstract

Some properties of gas mixtures, composed predominately of helium and lesser amounts of CO<sub>2</sub> and isobutane, were measured in a prototype drift chamber. The studies are motivated by the desire to reduce the multiple scattering inside the drift chamber at future high-luminosity, low-energy facilities such as  $\phi$  factories,  $\tau$ /charm factories, and B factories. The low atomic number of helium greatly reduces the multiple scattering contribution to the momentum resolution compared to an argon-based gas mixture. The position resolution, pulse height, efficiency, and breakdown characteristics were measured for various gas mixtures. A mixture of 83% He, 10% CO<sub>2</sub>, and 7% isobutane gives comparable results to that of an argon-based gas commonly used in drift chambers.

*Submitted to Nuclear Instruments and Methods A*

---

\*Work supported by Department of Energy contracts DE-AC03-76SF00515 (SLAC) and DE-AM03-76SF00010 (UCSC).

## 1. Introduction

Traditionally, the noble gas used in tracking devices in high-energy physics experiments has been argon because of its abundance, relatively low atomic number, low ionization potential and high gain. Now that we are entering the “factory” era of high-luminosity, low-energy facilities (such as  $\phi$  factories,  $\tau$ /charm factories and B factories), where the small statistical errors drive us to decrease systematic errors to unprecedented low values, we consider using noble gases with a lower atomic number, such as helium. With these gases, the multiple scattering contribution to the position resolution of tracking devices is significantly reduced. In addition, the probability of beam-related synchrotron photons interacting in the gas is significantly reduced, resulting in less background in the chamber which reduces wire aging and problems in track finding and triggering. Resolutions of  $260\ \mu\text{m}$  have been achieved in helium-propane mixtures [1], and recently measurements have been made on helium-DME and helium-CO<sub>2</sub>-isobutane mixtures [2,3]. In this paper, we describe our results on studies of helium-CO<sub>2</sub>-isobutane gas mixtures in a prototype drift chamber.

The momentum resolution  $\sigma_p$  of a charged particle with momentum component  $p$  perpendicular to the magnetic field in a homogeneous tracking system can be parametrized as follows: \*

$$\left(\frac{\sigma_p}{p^2}\right)^2 = A^2 + \left(\frac{B}{p}\right)^2,$$

---

\* Although drift chambers usually do not have uniformly distributed material or measurements, the parametrization is still useful for examining the general dependence of the resolution on measurement errors and multiple scattering.

where  $A$  is the contribution from spatial measurement errors and  $B/p$  is the contribution from multiple scattering. For a “typical” drift chamber,  $A$  is in the range (0.5 to 1.0)% / GeV/c. In a chamber with argon-based gas, the multiple-scattering term is typically around 0.7%/p. Since the charged-particle momentum spectra at future high-luminosity, low-energy facilities peak significantly below 1 GeV/c, the resolution is dominated by the multiple scattering term for most tracks if the drift chamber is filled with a traditional argon-based gas. By using a gas mixture with helium instead of argon, the radiation length of the gas mixture can be increased by a factor of at least six, which decreases the multiple-scattering contribution to the resolution by a factor of about 2.4.

During a workshop for an asymmetric-energy B factory [4], Monte Carlo studies were made on the effects of using a helium-based gas rather than an argon-based gas on four representative physics analyses. The conclusion in each case was that the physics measurements benefited significantly from the lower multiple scattering in a helium-based gas, even if the intrinsic spatial resolution is a factor of *two* worse.

Helium gas might be expected to give a poorer spatial resolution because of the smaller number of primary (and total) ion pairs along the path of a charged particle. The purpose of this study is to measure the resolution, as well as other properties, for a helium-based gas. We consider mixtures of helium, CO<sub>2</sub> (for limiting diffusion), and isobutane (for quenching). We measured the following

properties of various helium-based mixtures and, for comparison, an argon-based gas composed of 89% argon, 10% CO<sub>2</sub> and 1% methane, referred to as HRS gas:

- drift velocity as a function of electric field,
- pulse size,
- spatial resolution,
- breakdown characteristics, and
- efficiency.

## 2. Properties of the Gas Components

Properties of the individual gas components used in this study are listed in table 1, which shows the radiation length, and the number of primary and total electron-ion pairs per cm produced by a minimum ionizing particle. Since the radiation length of helium is so much larger than that of the other gases, the contribution of helium to the multiple scattering is almost negligible. However, the production of ion pairs is significantly lower in helium than in other gases.

The radiation length, the number of primary ion pairs/cm, and the total number of ions/cm for the gas mixtures considered in this study are given in table 2. The number of ions/cm *neglects* mechanisms such as the “Penning” effect which can increase the number of ions above the simple weighted sum over the individual components.

### 3. Measurements

#### 3.1 Experimental setup

Measurements of helium-based gases were conducted in a prototype drift chamber previously built to study a drift chamber for Mark II at SLC [7]. The prototype chamber is one-fifth of the full length of the Mark II chamber and consists of three super-layers corresponding to the fourth, fifth and sixth layers of the Mark II chamber. The wires in the middle super-layer are parallel to the central axis of the chamber, while those in the outer layers are inclined at approximately  $\pm 3.8^\circ$  to the axis. The active length of the wires is about 18 cm.

The drift cell has six sense wires spaced 8.33 mm apart, and a maximum drift distance of about 33 mm, as illustrated in fig. 1. The sense wires are 30  $\mu\text{m}$ -diameter, gold-plated tungsten, staggered by  $\pm 380 \mu\text{m}$  from the cell axis to provide left-right ambiguity resolution. A uniform electric drift field in the drift region is provided by voltages on a row of 19 field wires at each edge of the cell. Potential wires interspersed with the sense wires reduce signal coupling between the sense wires. A single high-voltage supply feeds a resistor chain that provides the necessary voltages for all the wires. Throughout this paper, when we report the *chamber voltage*, we are referring to the voltage at the top of this chain, which is approximately the same as the voltage on the outermost field wires in a super-layer. With this high-voltage scheme, the electric field and the gain both change as the chamber voltage is changed. The nominal chamber voltage of 4600 V used for HRS gas provides 4400 V at the central field wire, 1440 V on the potential wires, an electric field of 900 V/cm in the drift region, and a charge density of 14 pC/m on the sense wires.

The drift chamber signals are amplified in two stages with the same preamplifiers and postamplifiers as used on the Mark II drift chamber [8]. The time

between a cosmic-ray trigger (provided by scintillation counters above and below the chamber) and the drift-chamber pulse is digitized with LeCroy 2228A, 11-bit TDC's. The pulse area is integrated during a  $1\text{-}\mu\text{s}$  gate with LeCroy 2248W, 11-bit ADC's. A total of 24 wires are instrumented, but the measurements discussed here are based on the six sense wires in the central cell. The CAMAC modules are read out with a MAC II computer running KMAX<sup>TM</sup> software published by Sparrow. Approximately 2200 cosmic rays passing through the central cell of the chamber were recorded in about six hours.

The helium-based gas mixtures were mixed in the laboratory with commercial mass flow controllers, FloBox<sup>R</sup> from Sierra Instruments Inc. The gas-flow rate corresponded to about one chamber-volume change every two hours.

### 3.2 *Drift velocity*

In addition to the drift chamber, a separate small drift cell and a  $\beta$  source were used to measure the drift velocity of the helium-based gas as a function of electric drift field. The results of the measurements are shown in fig. 2, for both a representative helium-based mixture and for HRS gas. Note that the drift-velocity curve for the helium-based gas is not saturated, and hence the pressure and temperature of a chamber using this gas must be monitored or controlled to achieve high resolution. For an electric field of 1000 V/cm, the drift velocity is about  $25\ \mu\text{m}/\text{cm}$ , about half that for HRS gas.

### 3.3 *Pulse size*

The drift chamber signals were integrated with a LeCroy ADC module. The median of the ADC measurements is shown on a log plot as a function of chamber

voltage in fig. 3 for both HRS and the helium-based mixtures. (Recall that the nominal chamber voltage for HRS gas is 4600 V.) Note that the median pulse size has the exponential dependence on chamber voltage, or charge density on the sense wire, as expected.

Generally, increasing the amount of helium while decreasing the amount of  $\text{CO}_2$  results in a larger median pulse size for the same chamber voltage. A mixture of 83% helium, 10%  $\text{CO}_2$  and 7% isobutane has the same pulse area as HRS gas, for the same chamber voltage, despite the expectation that the total number of ion pairs produced per unit track length is about a factor of three lower (see table 2). It is unknown whether the pulse height is being increased by higher gain alone, or by the “Penning” effect in which metastable states in one gas (helium) transfer energy through collisions to other gases ( $\text{CO}_2$  or isobutane) which can ionize.

### *3.4 Chamber breakdown*

To study the dependence of chamber breakdown on gas mixture, we measured the rate at which the signal from a single sense wire fired a discriminator at a fixed threshold for different settings of the chamber voltage. The results are shown in fig. 4. For the helium mixtures in which the fraction of isobutane is kept constant at 7%, the breakdown voltages follow the same order as the chamber voltages corresponding to constant pulse size (see fig. 3). Mixtures with less helium and more  $\text{CO}_2$  break down at higher chamber voltages. When the amount of isobutane is decreased, the breakdown voltage also decreases. The HRS gas breaks down at a chamber voltage about 200 V less than the 83% helium, 10%  $\text{CO}_2$ , 7% isobutane mixture, even though they have the same median pulse height for the same chamber voltage.

### 3.5 Efficiency

To study the single-wire efficiency, triplets of neighboring sense wires were considered. We measured the probability that a single sense wire has a signal above a fixed threshold when its two nearest neighbors have such signals. This efficiency is plotted as a function of chamber voltage in fig. 5. Note the suppressed zero on the vertical scale. The chamber voltage at which the efficiency approaches 100% is directly correlated with the measured median pulse size (fig. 3), as expected. Note that HRS gas and the 83% helium, 10% CO<sub>2</sub>, 7% isobutane mixture have about the same efficiency and median pulse size for the same chamber voltage.

### 3.6 Resolution

For each track, the TDC timing information from the six wires in the cell was converted to spatial coordinates after resolving the left-right ambiguity. For HRS gas, which has relatively constant drift velocity in the drift region of the cell, a simple time-to-distance relation of the form

$$x = v(t - t_0)$$

was adequate, where  $x$  is the drift distance,  $v$  the drift velocity,  $t$  the TDC time, and  $t_0$  a constant relating the TDC start time of each channel to the trigger time for the event. The constant  $v$  was determined from the data by requiring that the maximum drift distance match the size of the cell (33 mm), while  $t_0$  was adjusted for each wire to center the residuals from track fits over many events.

For helium-based gases, the drift velocity is not constant but varies with the electric field  $E$  in the drift region of the cell, where  $E \approx 900$  V/cm. Even minor variations in  $E$ , such as that produced by the staggered sense wires, will modify



the drift time. A sense wire that is staggered toward the right side of the cell has a slightly higher(lower) electric field on the right(left) side of the cell, so the drift velocity is also slightly higher(lower) in the right(left) side of the cell. The time-to-distance relation needs a correction term to account for the resulting left-right difference in drift time. We chose the following empirical form

$$x = x_o \pm \delta \{1 - \exp[-(x_o/5)^2]\} \quad , \quad x_o = v(t - t_o) \quad ,$$

where the added term ranges from 0 near the wire to its maximum value  $\delta$  at large distances, and is about  $0.6 \delta$  at  $x = 5$  mm. The sign depends on the direction of stagger of the wire. It was found that values of  $\delta$  up to  $270 \mu\text{m}$  were needed for some gas mixtures.

The measured values of  $x$  from the six wires of each cosmic ray track were fit to straight lines. Tracks which had missing hits on any wire, or tracks with any residual larger than four times the expected resolution, were discarded. Also discarded were tracks having an angle greater than  $\pm 5^\circ$  from the sense wire plane. For the remaining tracks, the residuals were histogrammed, with a separate histogram for each millimeter interval in drift distance  $x$ . These residual distributions were fit to Gaussian distributions to determine the mean and standard deviation for each drift interval.

We quote the resolution as the standard deviations from the Gaussian fits scaled by  $\sqrt{6/4}$  to account for the loss of two degrees of freedom for the two parameters when fitting the six drift distances to a straight line. The resolution  $\sigma$  as a function of the drift distance  $x$  is shown in fig. 6 for HRS gas and a He:CO<sub>2</sub>:isobutane (83:10:7) mixture, both at a chamber voltage of 4800 V. Also shown as solid lines are the fits to a function containing a term for ion statistics near the wire

(which we approximate with an exponential), a constant term  $\sigma_o$ , and a diffusion term added in quadrature in the form

$$\sigma(x)^2 = a^2 e^{-2bx} + \sigma_o^2 + \sigma_d^2 x .$$

The exponential term is comparable for all gas mixtures studied, despite the fact that the estimated number of ion pairs per centimeter is significantly smaller for the helium mixtures (see table 2). Table 3 lists the measured values of  $\sigma_o$  and  $\sigma_d$  for all the gas mixtures. The dependence of resolution on drift distance is very comparable for HRS and for several helium mixtures.

The resolutions were also averaged over two different ranges of drift lengths: 8 mm and 24 mm. These ranges of drift distances were chosen because they correspond to the two cell sizes we were considering for an asymmetric  $B$  factory for small-cell and jet-cell geometries, respectively. The resolution is plotted as a function of chamber voltage in fig. 7 for HRS gas and for the helium-based mixtures. For all gases, the resolution for an 8-mm cell is slightly better than that of a 24-mm cell. The resolution improves with increasing chamber voltage until it reaches a minimum. At higher chamber voltages, the resolution degrades again. The values of  $\sigma_o$  and  $\sigma_d$  in table 3 correspond to a chamber voltage at which the resolution is minimized. At these voltages, the median pulse height is about the same for all gas mixtures.

### 3.7 Lorentz angle

Because the drift velocity is relatively low for the helium-based mixtures, the Lorentz angle in a magnetic field is also expected to be small. The expected Lorentz angle was calculated for the gas mixtures considered in this study with a computer

program [9] in which the Boltzmann transport equations are solved using the known elastic and inelastic cross sections for a number of pure gases. This program has given good agreement with experimental measurements for many gas mixtures.

This program predicts that a mixture of 83% helium, 10% CO<sub>2</sub>, and 7% isobutane will have a Lorentz angle of 15° for a magnetic field of 1 Tesla and an electric field of 1000 V/cm. HRS gas is predicted to have a Lorentz angle of 33° for the same conditions. A smaller Lorentz angle is particularly desirable for a small-cell drift chamber where a large Lorentz angle can lead to spiraling electron drift trajectories and, therefore, degraded resolution and poor efficiency for charged particles which traverse the edges of the cell.

#### 4. Conclusions

Our measurements on a mixture of 83% helium, 10% CO<sub>2</sub>, and 7% isobutane indicate that the efficiency, median pulse size, position resolution, and effects of diffusion are similar to those seen in the commonly used argon-based mixture (89% argon, 10% CO<sub>2</sub>, 1% methane) for the same charge density on the sense wire. We also find that the maximum operable high voltage setting for this helium-based gas is about 3.5% higher than that of the argon-based gas.

These results on helium-based gases are relevant for all low-energy facilities where particles of relatively low momenta are being measured, and the position resolution of tracks is dominated by multiple scattering. The radiation length of this helium mixture is almost eight times greater than the argon mixture, which significantly reduces the multiple scattering error. A helium-based gas is an obvious alternative to the traditional argon-based mixtures used in drift chambers.

## References

- [1] W. Zimmermann, V. Hepp, R. Kellogg, M. Schmitt, A. Skuja, A. Backer, C. Grupen, H. Suhr, G. Zech, N. Magnussen and H. Meyer, Nucl. Instr. Meth. A243 (1986) 86.
- [2] V. Cindro, H. Kolanoski, A. Lange, D. Lauterjung, F. Muller, T. Siegmund, W. Soder and H. Thurn, DO-E5-91-01 (1991).
- [3] S. M. Playfer, R. Bernet, R. A. Eichler, B. Stampfli, ETHZ-IMP-PR-91-3 (1991).
- [4] Workshop on Physics and Detector Issues for a High-Luminosity Asymmetric *B* Factory, SLAC-373 (1991).
- [5] Review of Particle Properties, Phys. Lett. B239 (1990).
- [6] F. Sauli, CERN Report 77-09 (1977).
- [7] G. Abrams et al., Nucl. Instr. Meth. A281 (1989) 55.
- [8] D. Briggs et al., IEEE Trans. on Nucl. Sci. NS-32, No. 1 (1985) 653.
- [9] Pashcal Coyle, LORENTZ program, UC Santa Cruz, unpublished.

**Table 1**

Radiation length  $X_0$  and primary and total ion-pair production [5,6] from a minimum ionizing particle for individual gas components used in mixtures in this study at atmospheric pressure and 20°C.

Gas Name	Symbol	Z	A	$X_0$ (m)	Primary Ions/cm	Total Ions/cm
helium	He	2	4	5690	5.9	7.8
methane	CH <sub>4</sub>	10	16	696	16	53
argon	Ar	18	40	118	29.4	94
carbon dioxide	CO <sub>2</sub>	22	44	196	34	91
isobutane	C <sub>4</sub> H <sub>10</sub>	34	58	182	46	195

**Table 2**

Radiation length  $X_0$ , and primary and total ion pair production for gas mixtures considered in this study at atmospheric pressure and 20°C, calculated using table 1.

Gas Mixture	$X_0$ (m)	Primary Ions/cm	Total Ions/cm
89% Ar, 10% CH <sub>4</sub> , (HRS gas)1% CO <sub>2</sub>	124	29.7	93.3
73% He, 20% CO <sub>2</sub> , 7% C <sub>4</sub> H <sub>10</sub>	652	14.3	37.5
78% He, 15% CO <sub>2</sub> , 7% C <sub>4</sub> H <sub>10</sub>	777	12.9	33.4
83% He, 10% CO <sub>2</sub> , 7% C <sub>4</sub> H <sub>10</sub>	960	11.5	29.2
88% He, 5% CO <sub>2</sub> , 7% C <sub>4</sub> H <sub>10</sub>	1258	10.1	25.1
82% He, 15% CO <sub>2</sub> , 3% C <sub>4</sub> H <sub>10</sub>	931	11.3	25.9
80% He, 10% CO <sub>2</sub> , 10% C <sub>4</sub> H <sub>10</sub>	833	12.7	34.8

**Table 3**

Results of a fit of the resolution  $\sigma$  versus drift distance  $x$  to a function of the form  $\sigma(x)^2 = a^2 e^{-2bx} + \sigma_o^2 + \sigma_d^2 x$ .

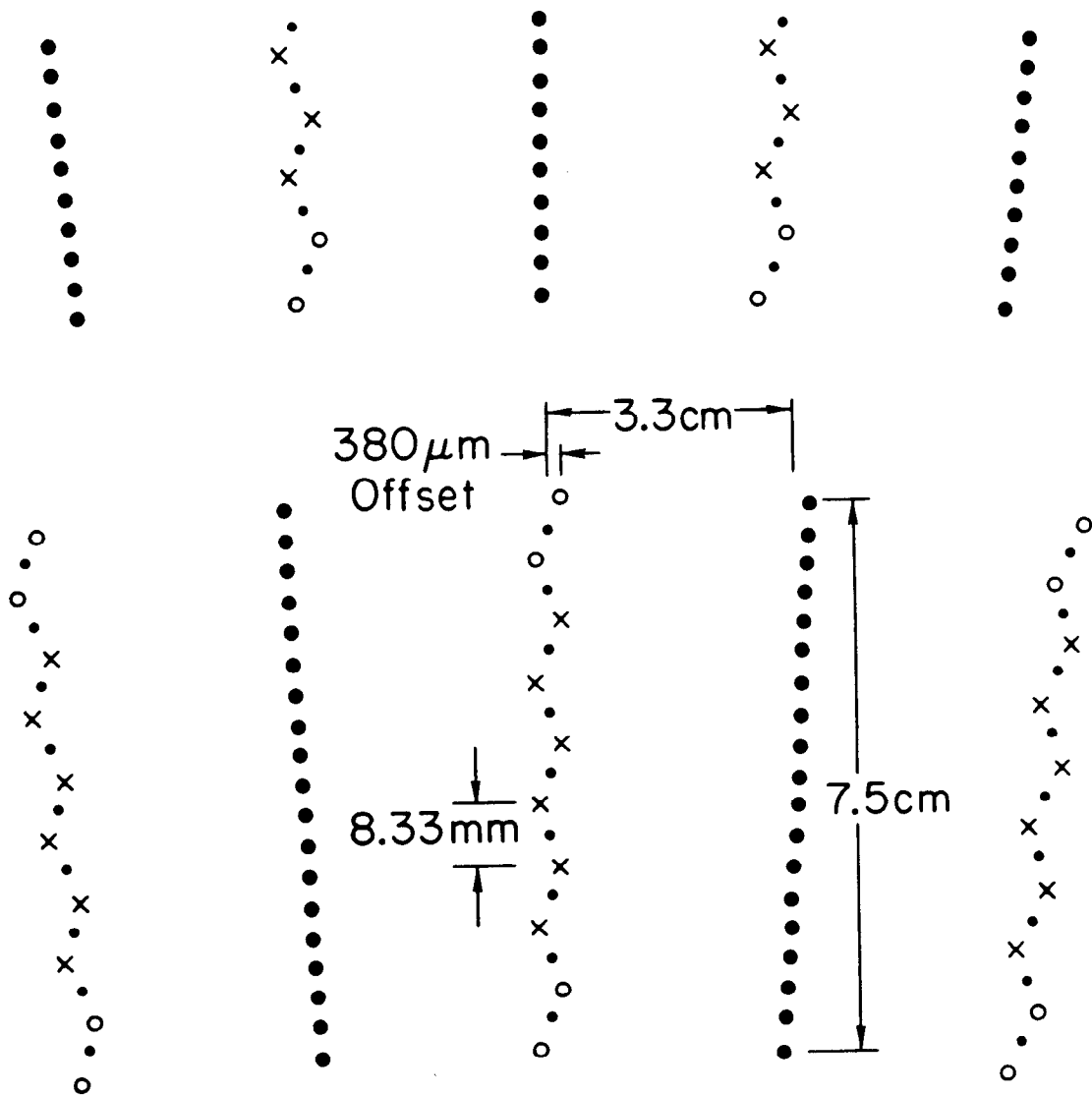
Gas Mixture	Chamber Voltage (V)	$\sigma_o$ ( $\mu\text{m}$ )	$\sigma_d$ ( $\mu\text{m}/\sqrt{\text{cm}}$ )
89% Ar, 10% CH <sub>4</sub> , 1% CO <sub>2</sub> (HRS gas)	4800	95 ± 4	109 ± 5
73% He, 20% CO <sub>2</sub> , 7% C <sub>4</sub> H <sub>10</sub>	5300	88 ± 8	109 ± 4
78% He, 15% CO <sub>2</sub> , 7% C <sub>4</sub> H <sub>10</sub>	5100	96 ± 7	109 ± 4
83% He, 10% CO <sub>2</sub> , 7% C <sub>4</sub> H <sub>10</sub>	4800	90 ± 8	110 ± 4
88% He, 5% CO <sub>2</sub> , 7% C <sub>4</sub> H <sub>10</sub>	4500	89 ± 9	131 ± 5
82% He, 15% CO <sub>2</sub> , 3% C <sub>4</sub> H <sub>10</sub>	4900	103 ± 12	133 ± 6
80% He, 10% CO <sub>2</sub> , 10% C <sub>4</sub> H <sub>10</sub>	5000	78 ± 12	105 ± 5

## Figure Captions

1. Cell configuration in the prototype drift chamber used in this study. The cell has six sense wires spaced 8.33 mm apart, and a maximum drift distance of about 33 mm.
2. Measured drift velocity as a function of electric drift field for a helium-based mixture and for HRS gas.
3. Measured median pulse size as a function of chamber voltage for the helium-based gases and for HRS gas.
4. Rate at which the signal from a single sense wire fires a fixed threshold discriminator as a function of chamber voltage for helium-based mixtures and for HRS gas. The symbols are defined in fig. 3.
5. Single-wire efficiency as a function of chamber voltage for helium-based mixtures and for HRS gas. The symbols are defined in fig. 3.
6. Measured resolution as a function of drift distance for HRS gas and for a helium-based mixture.
7. Resolution as a function of the voltage on the chamber for HRS gas and several helium-based mixtures. The average resolutions for drift distances up to 8 mm and up to 24 mm are shown.



# DRIFT CHAMBER WIRE PATTERN



× Sense Wire  
 • Potential Wire

○ Guard Wire  
 • Field Wire

3-83

4499A1

Fig. 1

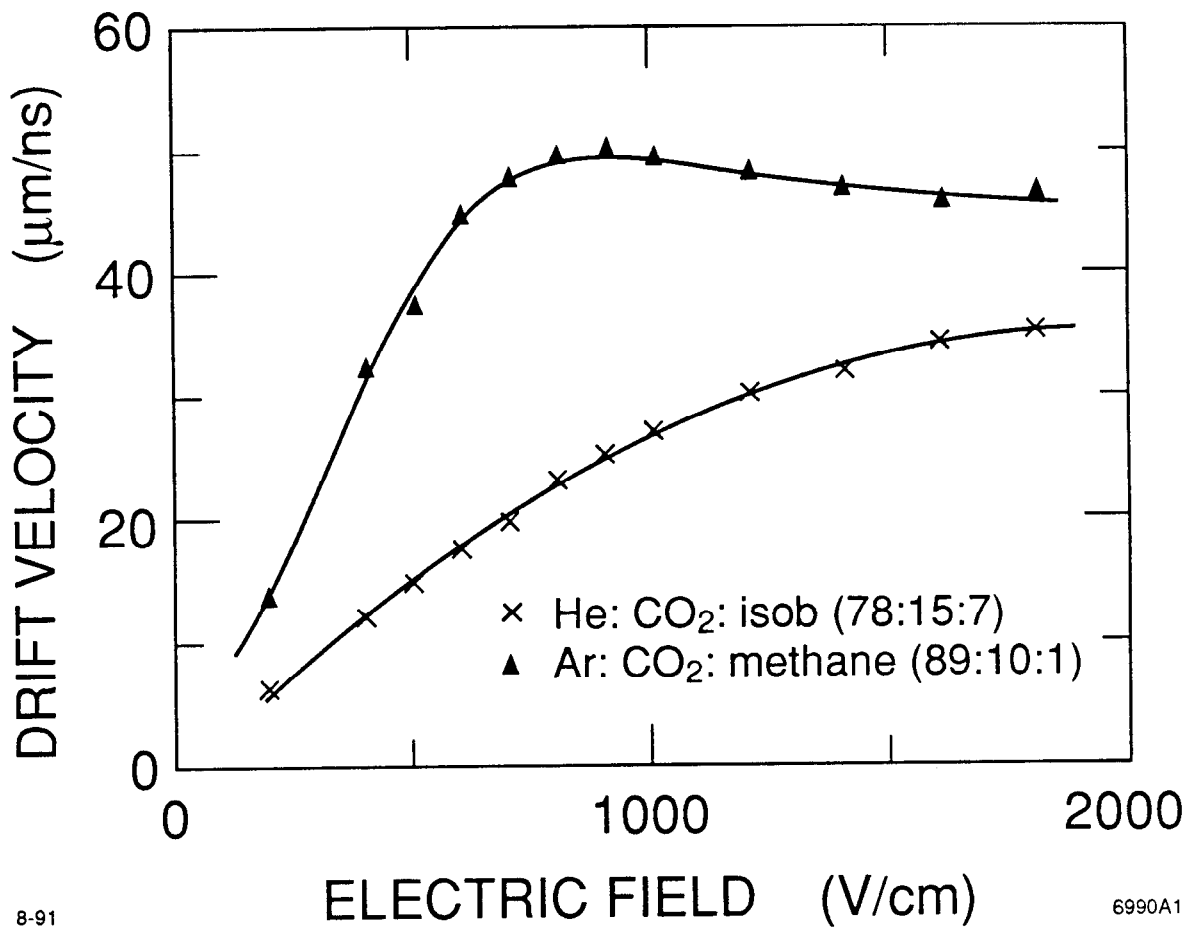
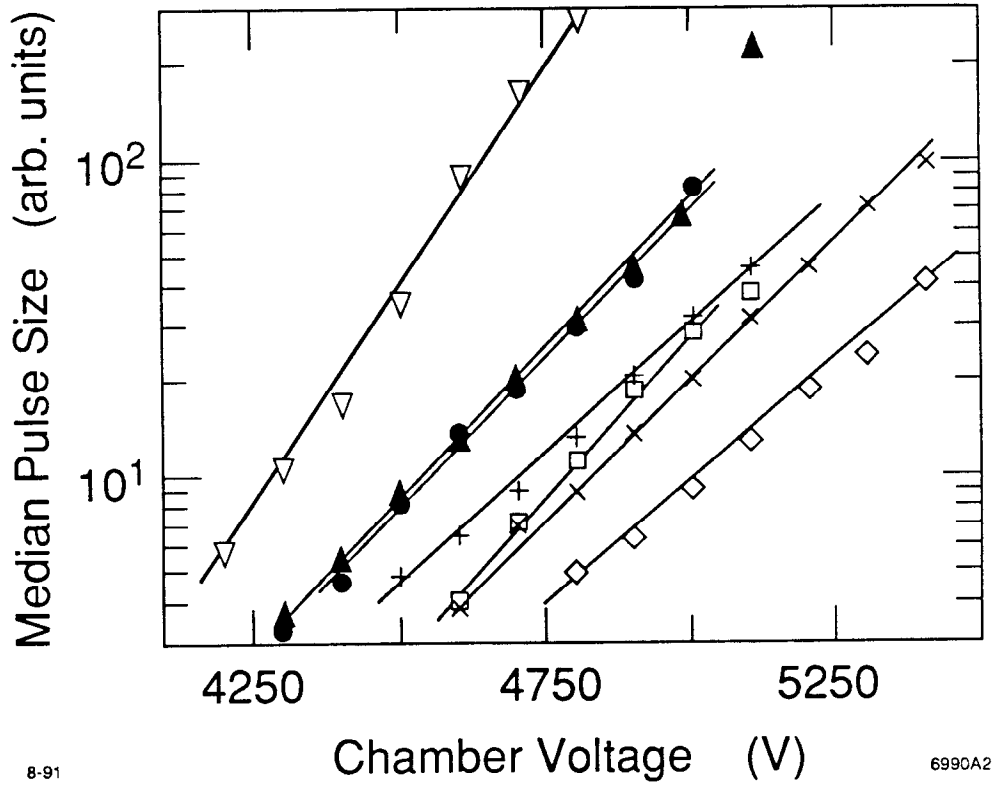


Fig. 2

	Helium	CO <sub>2</sub>	Isobutane
▽	88%	5%	} 7%
●	83%	10%	
×	78%	15%	
◇	73%	20%	
□	82%	15%	3%
+	80%	10%	10%
	Argon	CO <sub>2</sub>	Methane
▲	89%	10%	1%



8-91

6990A2

Fig. 3

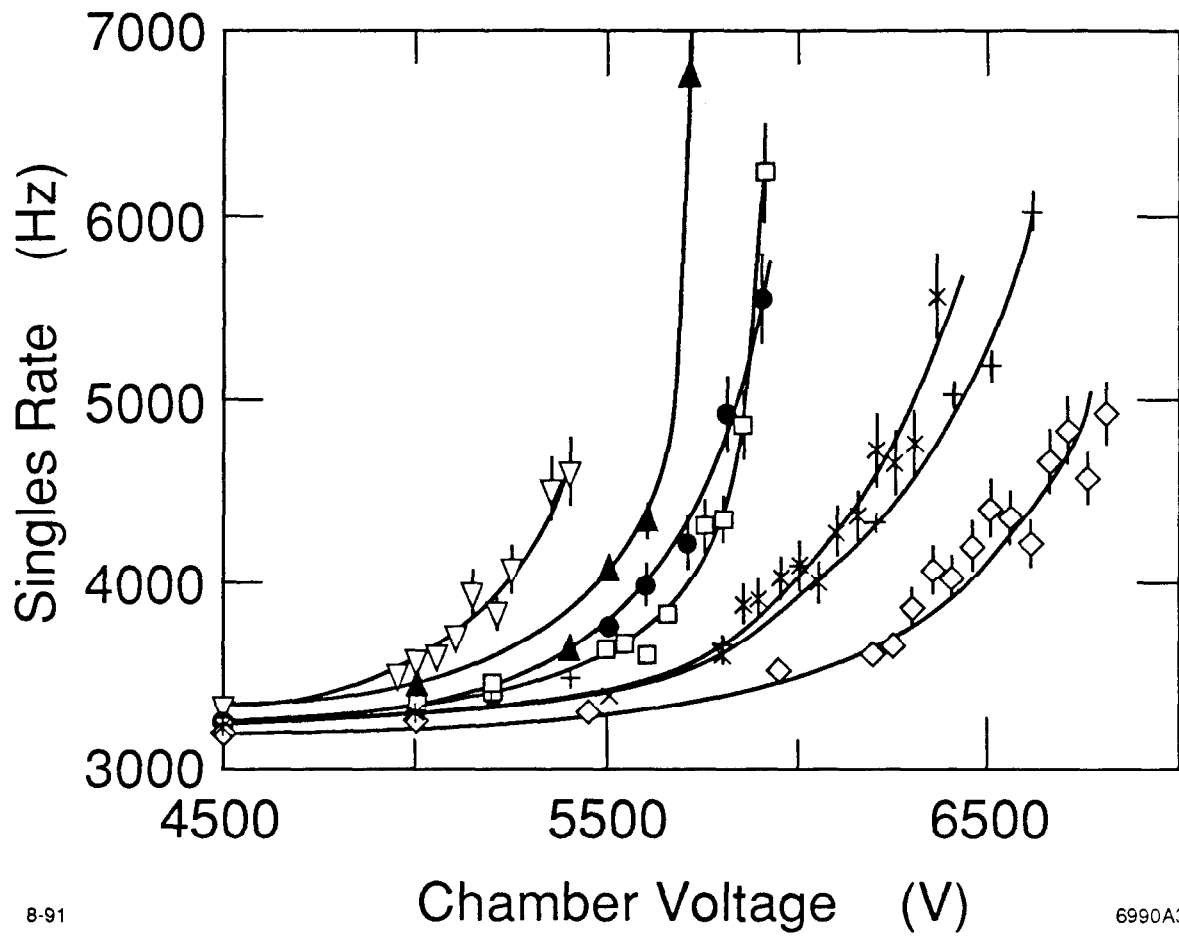


Fig. 4

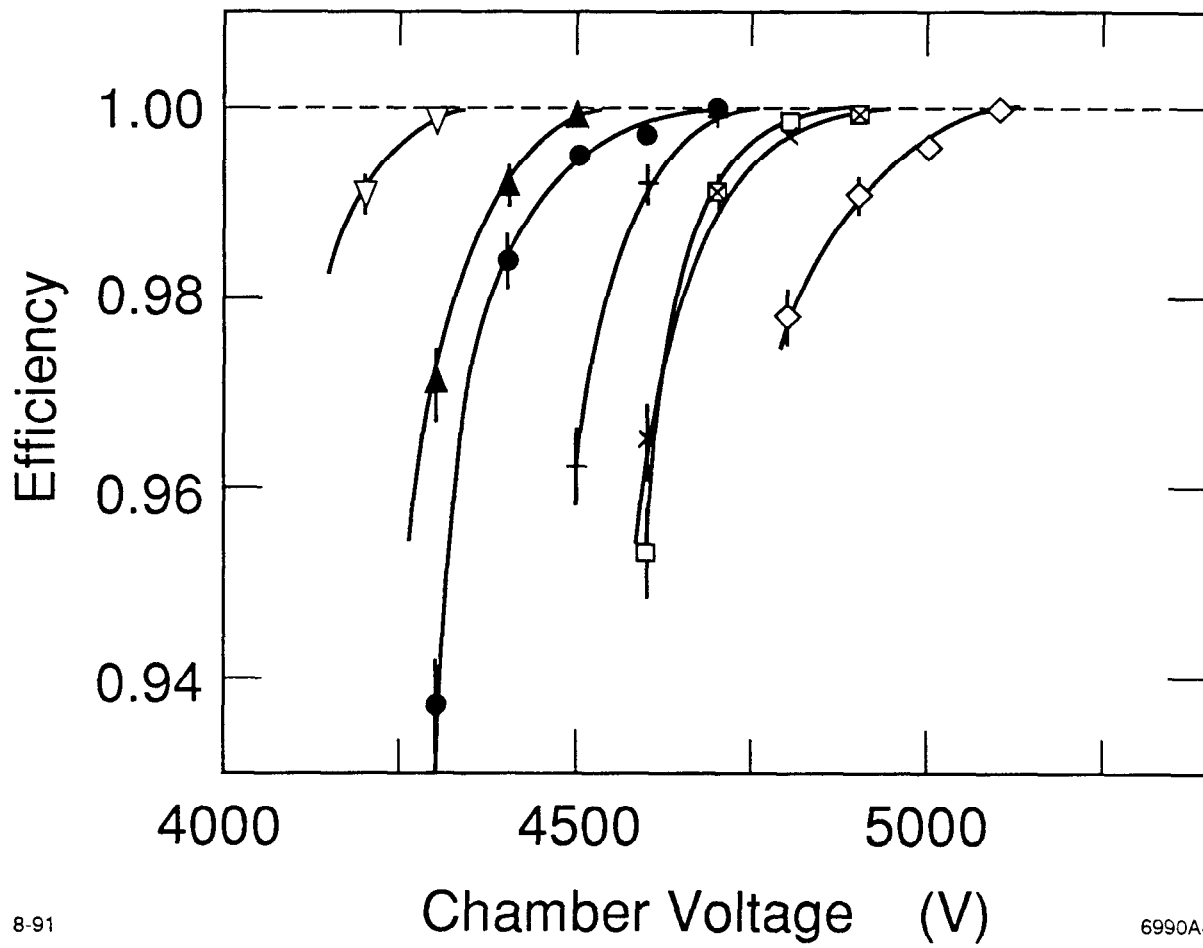


Fig. 5

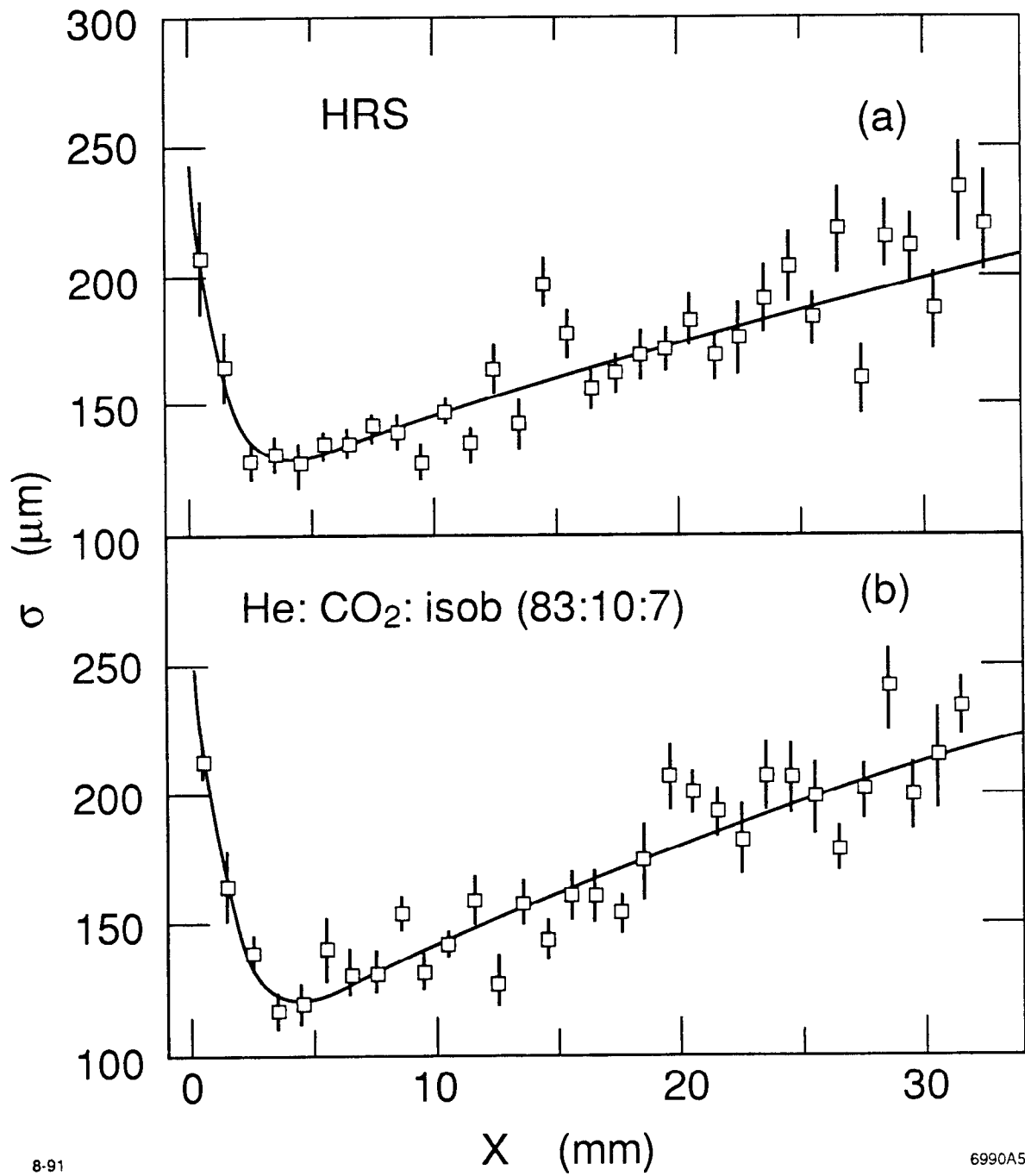


Fig. 6

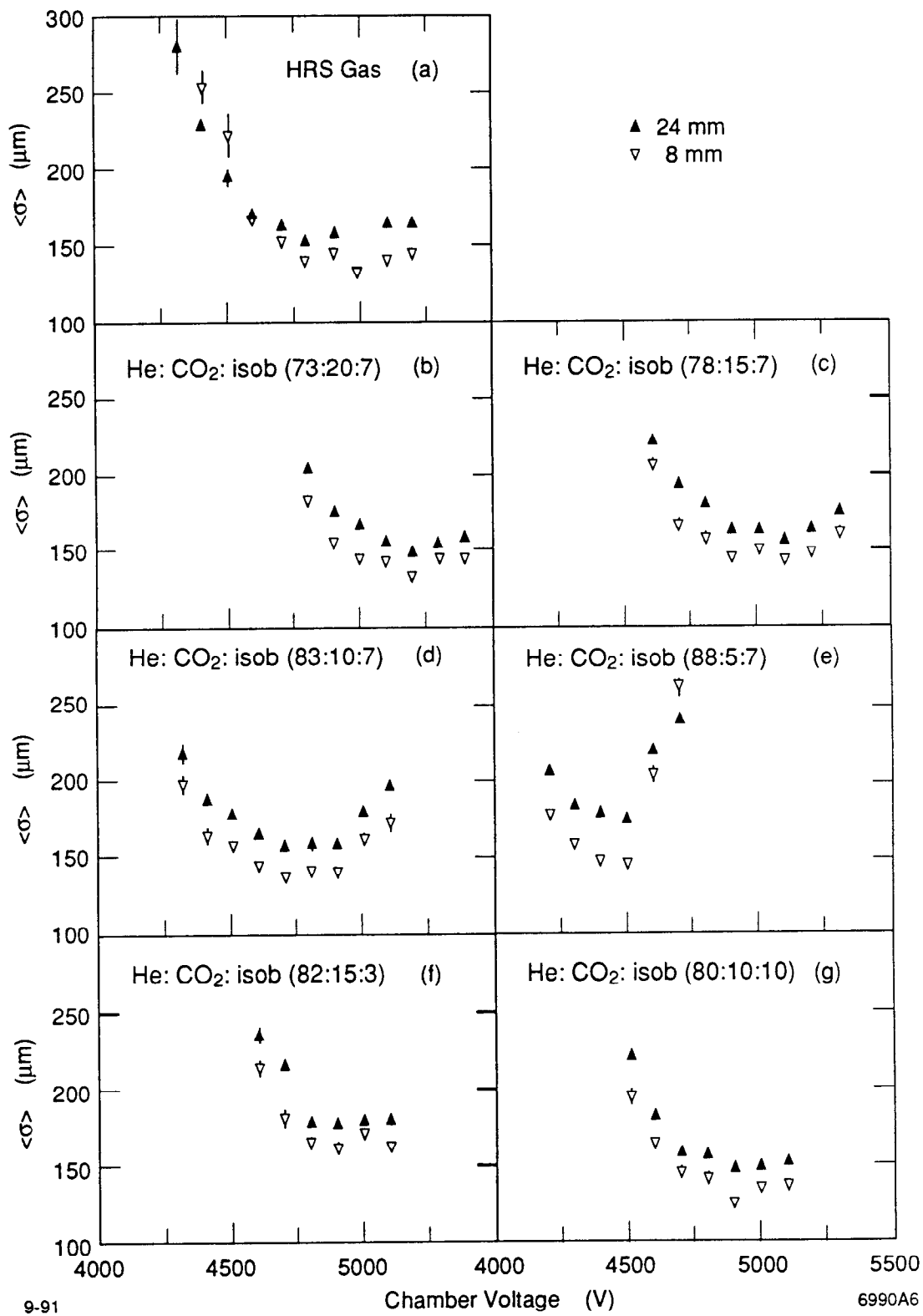


Fig. 7